

Bremsstrahlung on noble gases at low energies

A.I. Milstein,^{1,2,*} S.G. Salnikov,^{1,2,†} and M.G. Kozlov^{3,4,‡}

¹*Budker Institute of Nuclear Physics of SB RAS, 630090 Novosibirsk, Russia*

²*Novosibirsk State University, 630090 Novosibirsk, Russia*

³*Petersburg Nuclear Physics Institute of NRC “Kurchatov Institute”, 188300 Gatchina, Russia*

⁴*St. Petersburg Electrotechnical University “LETI”,*

Prof. Popov Str. 5, 197376 St. Petersburg, Russia

(Dated: July 13, 2022)

A detailed analysis of the bremsstrahlung spectrum at nonrelativistic electron scattering on argon and xenon is carried out. It is shown that the approximate formulas widely used for the description of bremsstrahlung spectra lead to predictions that significantly differ from the exact results. In the limit when the photon frequency tends to zero, a rigorous proof of the relationship between the spectrum of the bremsstrahlung with a transport cross section of electron scattering on an atom is given. This proof does not require any assumptions about the dependence of the scattering phases on energy. For electron energies lower than the luminescence threshold, it is shown that the predictions for a number of radiated photons obtained by the exact formula are in good agreement with the available experimental data.

I. INTRODUCTION

In recent years, search for particles of dark matter has stimulated the development of detectors with increased sensitivity to registration of such particles [1–5]. One of the fundamental processes, that determine the properties of new detectors, is bremsstrahlung on noble gases, in particular on argon or xenon. Many years ago approximate formulas for describing the bremsstrahlung process at low energies were suggested [6, 7]. In these formulas, the bremsstrahlung spectrum is expressed in terms of the electron scattering cross section on an atom. These approximate formulas were used to compare experimental data with

* A.I.Milstein@inp.nsk.su

† S.G.Salnikov@inp.nsk.su

‡ kozlov_mg@pnpi.nrcki.ru

theory. In Ref. [8] it was noted that the region of applicability of the approximate formulas is not defined. In particular, it is not clear whether these formulas can be used to describe bremsstrahlung spectrum on noble gases, since in this case the Ramsauer effect [9] appears.

In our work, we carry out a detailed comparison of the bremsstrahlung spectra of nonrelativistic electron on argon and xenon obtained by the exact and approximate formulas. Exact formulas have been known for a long time (see, e.g., Refs. [10, 11] and references therein). In the limit when the photon frequency ω tends to zero, the bremsstrahlung spectrum is expressed in terms of the transport cross section in the process of elastic scattering of an electron on an atom. However, the proof of this statement for nonrelativistic electrons was obtained only in various approximations [12–15]. For instance, the Born approximation or the approximation in which the contribution of the s -wave to the scattering cross section is dominant were discussed. We present for the first time a rigorous proof of the relationship between the bremsstrahlung spectrum and the transport cross section at $\omega \rightarrow 0$ and arbitrary energies of the incident electron (compared to the energies of atomic electrons). In addition, it is shown that the approximate formulas used in the literature for the bremsstrahlung spectrum at finite photon frequencies give predictions that differ significantly from the exact results. We use the results for the spectrum for comparison of the predictions for a number of emitted photons in a certain wavelength region with the experimental results [1–5].

II. THEORY

Let us consider the process of bremsstrahlung at the scattering of a nonrelativistic electron with kinetic energy ε on an atom. For an electron wave function, we use the partial wave expansions

$$\psi^{(\pm)}(\mathbf{r}) = \frac{1}{2p} \sum_{l=0}^{\infty} (2l+1) i^l e^{\pm i\delta_l} R_l(p, r) P_l(\cos \theta), \quad (1)$$

where $p = \sqrt{2m\varepsilon}$ is the electron momentum, δ_l are the scattering phases, P_l are the Legendre polynomials, and $R_l(p, r)$ are the radial wave functions having asymptotics at large distances

$$R_l(p, r) \xrightarrow{r \rightarrow \infty} \frac{2}{r} \sin \left(pr - \frac{\pi l}{2} + \delta_l \right). \quad (2)$$

The function $\psi^{(+)}(\mathbf{r})$ contains at large distances the plane wave and a divergent spherical wave, while $\psi^{(-)}(\mathbf{r})$ contains the plane wave and a convergent spherical wave. Then,

the bremsstrahlung spectrum in the nonrelativistic approximation has the form (see, e.g., Ref. [11] and Appendix)

$$\begin{aligned} \frac{d\sigma}{d\omega} &= \frac{2\alpha p_f}{3\omega p_i} \sum_{l=0}^{\infty} (l+1) (|M_{l,l+1}(p_f, p_i)|^2 + |M_{l+1,l}(p_f, p_i)|^2), \\ M_{l',l}(p_f, p_i) &= \frac{\exp\{i[\delta_l(p_i) + \delta_{l'}(p_f)]\}}{p_i p_f} \int_0^{\infty} r^2 dr R_{l'}(p_f, r) \frac{\partial U}{\partial r} R_l(p_i, r), \end{aligned} \quad (3)$$

where α is the fine-structure constant, $\omega = \varepsilon_i - \varepsilon_f$ is the emitted photon frequency, ε_i and ε_f are the electron energies before and after collision, $U(r)$ is the electron potential energy in an atomic field, $\hbar = c = 1$. Below we will refer Eq. (3) as the exact formula in contrast to various approximations to this result.

For $\omega \ll \varepsilon_i$ the expression (3) is noticeably simplified:

$$\frac{d\sigma}{d\omega} = \frac{4\alpha}{3\omega} \sum_{l=0}^{\infty} (l+1) |M_{l,l+1}(p_i, p_i)|^2. \quad (4)$$

The matrix element

$$T_l(p) = M_{l,l+1}(p, p) = \frac{\exp\{i[\delta_l(p) + \delta_{l+1}(p)]\}}{p^2} \int_0^{\infty} r^2 dr R_l(p, r) \frac{\partial U}{\partial r} R_{l+1}(p, r) \quad (5)$$

can be expressed in terms of the scattering phases δ_l for any momenta p . To prove this statement, we use the relations

$$\begin{aligned} \frac{\partial U}{\partial r} &= i[\mathcal{P}_r, H_l] + \frac{l(l+1)}{mr^3}, \\ H_{l+1} - H_l &= \frac{l+1}{mr^2}, \\ H_l &= \frac{\mathcal{P}_r^2}{2m} + U(r) + \frac{l(l+1)}{2mr^2}, \end{aligned} \quad (6)$$

where $\mathcal{P}_r = -i\left(\frac{1}{r} + \frac{\partial}{\partial r}\right)$ is the radial momentum operator, H_l is the radial Hamiltonian for an electron in a state with orbital momentum l , and m is the electron mass. However, it is impossible to use the hermiticity of the Hamiltonian in Eq. (5) and make the replacement

$$\int_0^{\infty} r^2 dr R_l(p, r) [\mathcal{P}_r, H_l] R_{l+1}(p, r) \implies - \int_0^{\infty} r^2 dr R_l(p, r) \mathcal{P}_r \frac{l+1}{mr^2} R_{l+1}(p, r),$$

since the integral is conditionally convergent. To overcome this difficulty, we use the trick described in [16, 17]. Consider the regularized matrix element

$$\tilde{T}_l(p) = \frac{\exp\{i[\delta_l(p) + \delta_{l+1}(p)]\}}{p^2} \int_0^{\infty} r^2 dr R_l(p, r) \frac{\partial U}{\partial r} R_{l+1}(p, r) e^{-\lambda r}, \quad (7)$$

where $\lambda \rightarrow 0$. In the expression for $\widetilde{T}_l(p)$, the hermiticity of the Hamiltonian can already be used. Neglecting the terms quadratic in λ in pre-exponent and still keeping $e^{-\lambda r}$ in the integrand, we reduce the matrix element to the form

$$\begin{aligned}\widetilde{T}_l(p) &= \exp \{i[\delta_l(p) + \delta_{l+1}(p)]\} \cdot (t_1 + t_2), \\ t_1 &= \frac{l+1}{2mp^2} \int_0^\infty dr e^{-\lambda r} \left[R'_l R_{l+1} - R_l R'_{l+1} + \frac{2(l+1)}{r} R_l R_{l+1} \right], \\ t_2 &= -\frac{\lambda}{p^2} \int_0^\infty r^2 dr e^{-\lambda r} \left[R_l \frac{\mathcal{P}_r^2}{2m} R_{l+1} - R_{l+1} \frac{\mathcal{P}_r^2}{2m} R_l \right],\end{aligned}\quad (8)$$

where $R'_L = \partial R_L / \partial r$. Note that the factor $e^{-\lambda r}$ in the integrand for t_1 can be omitted since the integral is already absolutely convergent. Using the radial Schrödinger equation for the wave functions R_l and R_{l+1} , we obtain the relation

$$R'_l R_{l+1} - R'_{l+1} R_l + \frac{2(l+1)}{r} R_l R_{l+1} = \frac{\partial}{\partial r} \left[r (R'_{l+1} R_l - R'_l R_{l+1}) \right]. \quad (9)$$

Therefore, the contribution of t_1 vanishes,

$$t_1 = \frac{l+1}{2mp^2} \int_0^\infty dr \left[R'_l R_{l+1} - R_l R'_{l+1} + \frac{2(l+1)}{r} R_l R_{l+1} \right] = 0. \quad (10)$$

Since the matrix element t_2 is proportional to the small factor λ , this factor can only be compensated by the contribution to the integral of large distances r . Therefore, we can use the asymptotics (2) of the wave functions and replace $\frac{\mathcal{P}_r^2}{2m}$ by ε . As a result, in the limit $\lambda \rightarrow 0$ we obtain

$$\begin{aligned}t_2 &= -\frac{8\lambda\varepsilon}{p^2} \int_0^\infty dr e^{-\lambda r} \sin \left(pr - \frac{\pi l}{2} + \delta_l \right) \sin \left(pr - \frac{\pi(l+1)}{2} + \delta_{l+1} \right) \\ &= \frac{2}{m} \sin(\delta_l - \delta_{l+1}).\end{aligned}\quad (11)$$

Hence, the matrix element (5) reads

$$T_l(p) = \frac{2}{m} \sin(\delta_l - \delta_{l+1}) \exp \{i[\delta_l(p) + \delta_{l+1}(p)]\}. \quad (12)$$

Using Eq. (12), we arrive at the expression for the asymptotics of the bremsstrahlung spectrum at $\omega \rightarrow 0$:

$$\frac{d\sigma}{d\omega} = \frac{16\alpha}{3\omega m^2} \sum_{l=0}^{\infty} (l+1) \sin^2(\delta_l - \delta_{l+1}). \quad (13)$$

This formula can be expressed in terms of the transport scattering cross section σ_{tr} of an electron on an atom,

$$\sigma_{\text{tr}} = \frac{4\pi}{p^2} \sum_{l=0}^{\infty} (l+1) \sin^2(\delta_l - \delta_{l+1}). \quad (14)$$

Finally, we obtain the bremsstrahlung spectrum for low frequencies

$$\frac{d\sigma}{d\omega} = \frac{8\alpha}{3\pi\omega} \frac{\varepsilon}{m} \sigma_{\text{tr}}. \quad (15)$$

In some papers (see [8, 15] and references therein), to describe the bremsstrahlung spectrum for arbitrary frequencies ω , the formula

$$\frac{d\sigma}{d\omega} = \frac{4\alpha}{3\pi m\omega} \frac{p_i}{p_f} [\varepsilon_i \sigma(\varepsilon_f) + \varepsilon_f \sigma(\varepsilon_i)], \quad (16)$$

was applied. This formula coincides with (15) in the limit $\omega \rightarrow 0$, if the transport cross section is used as σ . Similar expression in terms of the scattering cross section is widely used to describe the cross section of photon absorption which is the inverse process to bremsstrahlung. Besides, in most of cases the authors used only the contribution of s -wave [6, 8, 18, 19], or used as σ the cross section of elastic scattering by an atom [1–4, 7],

$$\sigma_{\text{el}} = \frac{4\pi}{p^2} \sum_{l=0}^{\infty} (2l+1) \sin^2 \delta_l. \quad (17)$$

In Refs. [5, 12] the relationship (16) between the bremsstrahlung spectrum and the transport cross section was pointed out, but the authors of these works supposed that using of an elastic cross section is also admissible. However, the cross sections σ_{el} and σ_{tr} in the case of noble gases differ significantly even for the energy of the incident electron much less than the energy of atomic electrons (see Fig. 1). Note that the minimum in the cross sections is a consequence of the Ramsauer effect, which manifests in a nontrivial energy dependence of the scattering phase δ_0 at low-energy electron scattering on noble gases [20–26]. For example, δ_0 vanishes at the electron energy 0.3 eV in the case of argon and 0.8 eV in the case of xenon.

III. RESULTS AND DISCUSSION

For a quantitative description of the bremsstrahlung spectrum and the electron scattering cross section in the cases of argon and xenon, we use the potential energy $U(r)$ as a sum

$$U(r) = U_{\text{st}}(r) + U_{\text{pol}}(r),$$

$$U_{\text{pol}}(r) = - \left[\frac{\alpha_d}{(\rho^2 + d^2)^2} + \frac{\alpha_q}{(\rho^3 + d^3)^2} \right] \text{Ry}, \quad \rho = \frac{r}{a_B}, \quad (18)$$

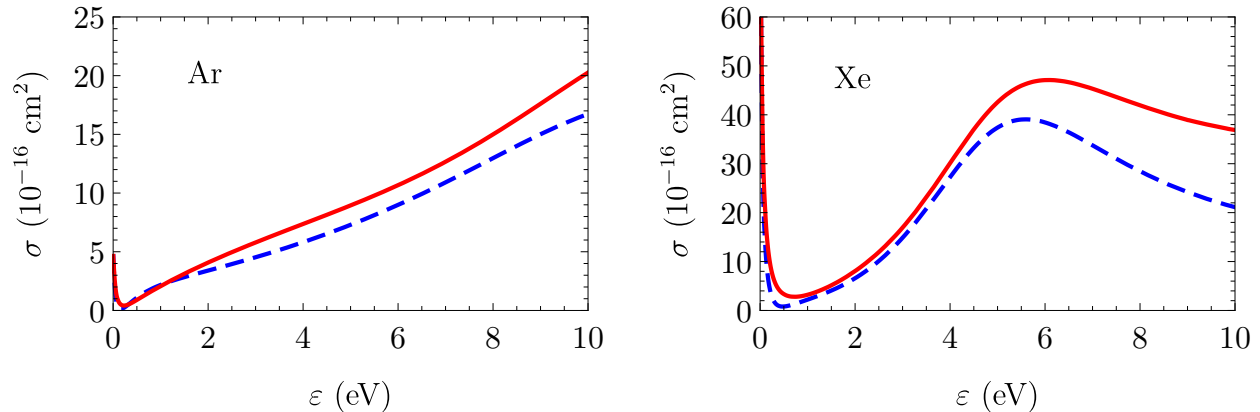


Figure 1. Cross sections for electron scattering on argon and xenon atoms calculated using the potential (18). The solid line corresponds to the elastic scattering cross section σ_{el} , and the dashed line corresponds to the transport cross section σ_{tr} .

	α_d	α_q	d
Ar	13.9	60.5	1.95
Xe	30.5	134.7	2.13

Table I. The dimensionless parameters of the polarization potential (18).

where U_{st} is a static potential determined by the charge distribution in the atom, U_{pol} is a polarization potential, $\text{Ry} = me^4/2\hbar^2$, $a_B = \hbar^2/me^2$, e is the electron charge. The values of the dimensionless parameters of the polarization potential α_d , α_q and d used in our paper provide agreement between theoretical predictions for the elastic electron scattering cross section with experimental data [27]. These values are given in the Table I. Note that an account for the polarization potential is very important for correct description of the scattering cross section in the case of noble gases due to large values of the parameters α_d and α_q . The static potential U_{st} was calculated using the Hartree-Fock-Dirac method [28].

The bremsstrahlung spectra on argon and xenon, obtained by means of the exact (3) and approximate (16) formulas, are shown in Fig. 2 for energies $\varepsilon = 0.5 \div 10$ eV. It is seen that the applicability of the approximate formulas for the description of the bremsstrahlung spectrum in the specified energy region is very limited. Note that at low photon frequencies agreement of the exact formula with the approximate formula based on the transport cross section σ_{tr} is much better than with the approximate formula based on σ_{el} .

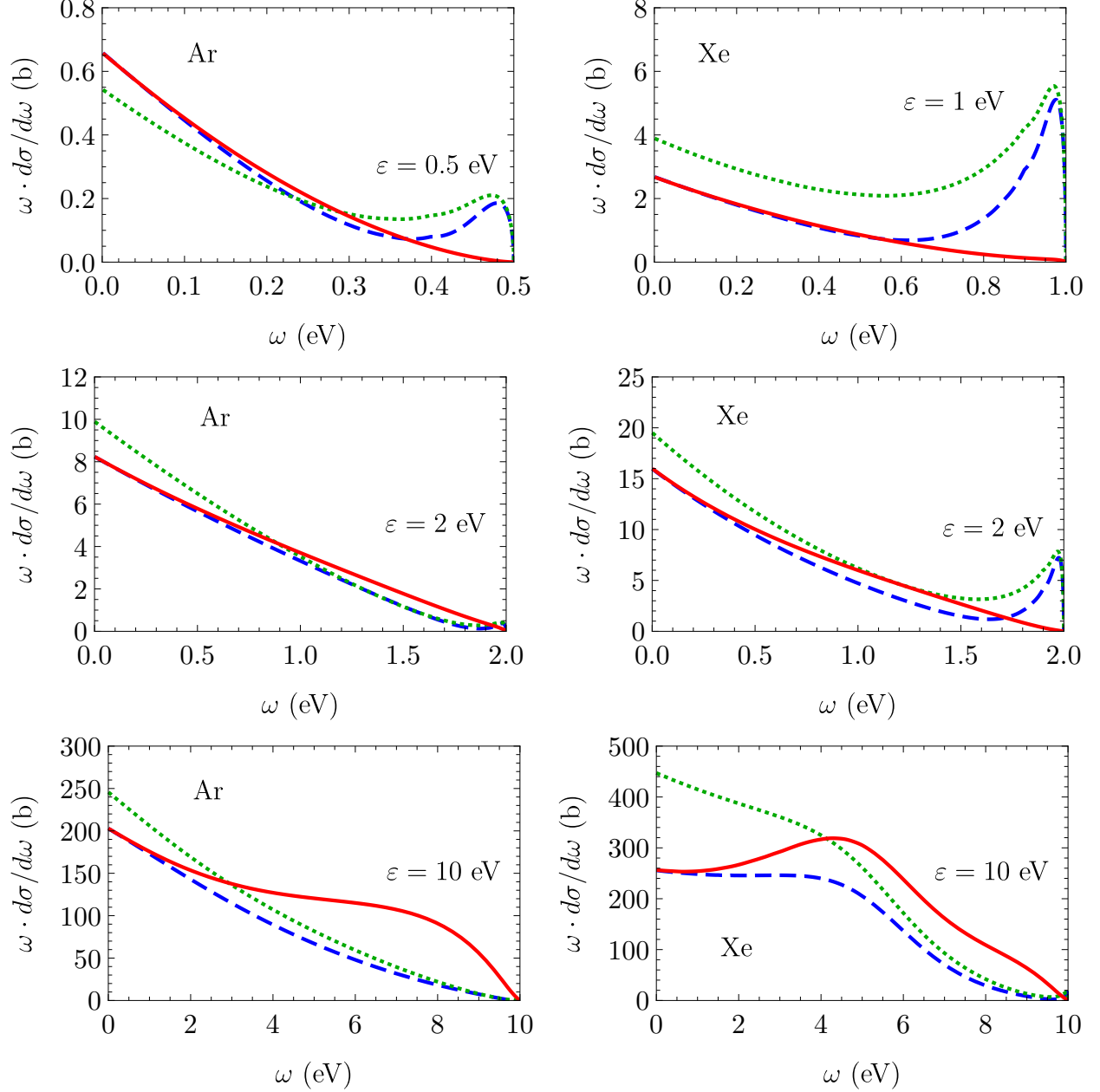


Figure 2. The frequency dependence of $\omega \cdot d\sigma/d\omega$ for scattering of electrons on argon and xenon atoms. The solid line corresponds to the exact formula (3), the dashed line corresponds to Eq. (16) expressed in terms of the transport cross section σ_{tr} , while the dotted line corresponds to Eq. (16) expressed through σ_{el} .

In Refs. [1–5] experimental data for the number of emitted photons are given for electrons accelerated in an electric field and scattered on argon or xenon atoms. In this case, photons were registered in the wavelength region $\lambda = 0 \div 1000$ nm for argon and $\lambda = 120 \div 1000$ nm

for xenon. Reduced yield of bremsstrahlung photons \mathcal{N}_γ , which is defined as the number of bremsstrahlung photons per electron per atomic concentration and per drift path, is given by

$$\mathcal{N}_\gamma = \int_{\lambda_{\min}}^{\lambda_{\max}} d\lambda \int_{\omega}^{\infty} d\varepsilon \frac{v_e}{v_d} \frac{d\sigma}{d\omega} \frac{d\omega}{d\lambda} f(\varepsilon), \quad (19)$$

where $v_e = \sqrt{2\varepsilon/m}$ is the electron velocity, v_d is the drift velocity, $f(\varepsilon)$ is the electron distribution function normalized as

$$\int_0^{\infty} d\varepsilon f(\varepsilon) = 1. \quad (20)$$

The electron distribution function and the drift velocity are determined by the magnitude of the electric field. For these values, we used the results obtained by means of EEDF [29]. The dependence of \mathcal{N}_γ on the ratio \mathcal{E}/N , where \mathcal{E} is the electric field and N is the concentration of atoms, is shown in Fig. 3. For the reduced electric field, we use conventional units $1 \text{ Td} = 10^{-17} \text{ V} \cdot \text{cm}^2$. It is seen that the predictions for \mathcal{N}_γ , obtained from the exact formulas, significantly differ from those obtained using approximate formulas. Note that this difference essentially depends on the region of integration over wavelengths in Eq. (19). The experimental data for the photon yield at values \mathcal{E}/N , which lead to emission of photons below the threshold of electroluminescence, are also shown in Fig. 3. Above this threshold, the photon yield due to electroluminescence significantly exceeds the photon yield due to bremsstrahlung. It is important that the predictions obtained from the exact formula are in much better agreement with the experimental data than obtained by approximate formulas. This is especially noticeable in the case of xenon.

IV. INFLUENCE OF POLARIZATION RADIATION

When nonrelativistic electrons are scattered by an atom without excitation of atomic electrons, the emission of photons is related not only to the radiation of the incident electron (bremsstrahlung) but also to the radiation of atomic electrons in the intermediate states (polarization radiation, see [14, 15]). In this case, if the energy of the incident electron is comparable to the interval between atomic levels, then the phenomenon of electroluminescence occurs. The intensity of radiation due to electroluminescence significantly exceeds the intensity of bremsstrahlung. Therefore, it is important to discuss the effect of polarization radiation on the photon spectrum below the electroluminescence threshold.

Assuming that the main contribution to the amplitude of polarization radiation is given by the motion of incident electron at large distances compared to an atomic size, the total amplitude of the photon emission below the threshold of electroluminescence can be written as

$$M_{V,l}(p_f, p_i) = \frac{\exp\{i[\delta_l(p_i) + \delta_{V'}(p_f)]\}}{p_i p_f} \int_0^\infty r^2 dr R_{V'}(p_f, r) \left[\frac{\partial U}{\partial r} - \frac{\alpha_d a_B^3 m \omega^2}{r^2} \right] R_l(p_i, r), \quad (21)$$

where α_d is the static polarizability which coincides with that given in the Table I. In Eq. (21) ω is small compared to the resonant frequency (luminescence frequency). As should be, at $\omega \rightarrow 0$ the contribution of polarization radiation vanishes. Since the contribution of polarization radiation in Eq. (21) was obtained under the assumption $r \gg a_B$, account for the distances of the order $r \sim a_B$ requires a special consideration. For a qualitative discussion, we replace a_B^2/r^2 in the polarization contribution by $1/(\rho^2 + d^2)$ in the same way as in Eq. (18), where $\rho = r/a_B$. Comparison of theoretical predictions with and without account for the polarization radiation and the experimental data is given in Fig. 4 for the case of argon. It is seen that account for the polarization radiation in the near-threshold region noticeably improves the agreement between theory and experiment.

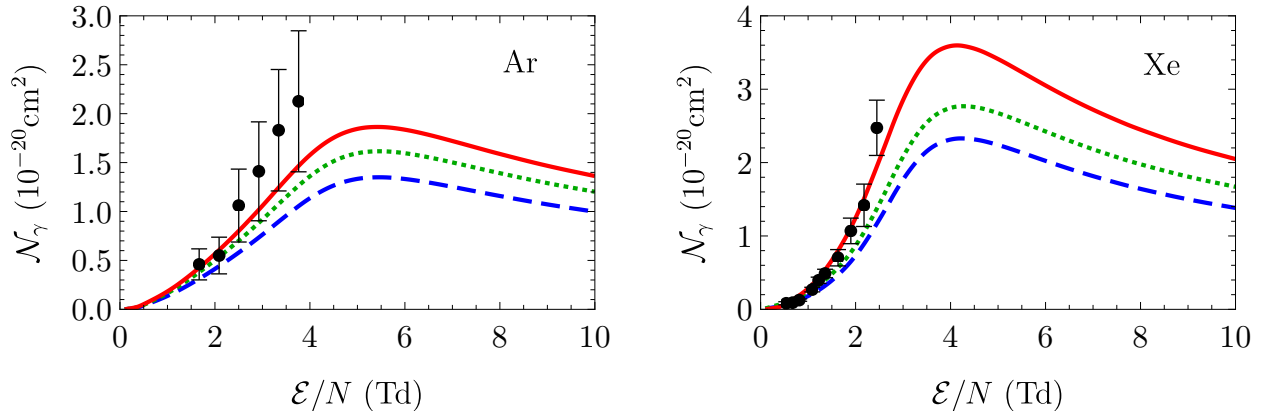


Figure 3. The reduced yield of bremsstrahlung photons as a function of the reduced electric field for argon and xenon. Theoretical predictions are obtained by means of Eq. (19). The solid line corresponds to the exact formula (3) for $d\sigma/d\omega$, the dashed line corresponds to Eq. (16) expressed in terms of the transport cross section σ_{tr} , while the dotted line corresponds to Eq. (16) expressed via σ_{el} . Experimental data for argon are taken from Ref. [3], and data for xenon are recalculated from that in Ref. [5].

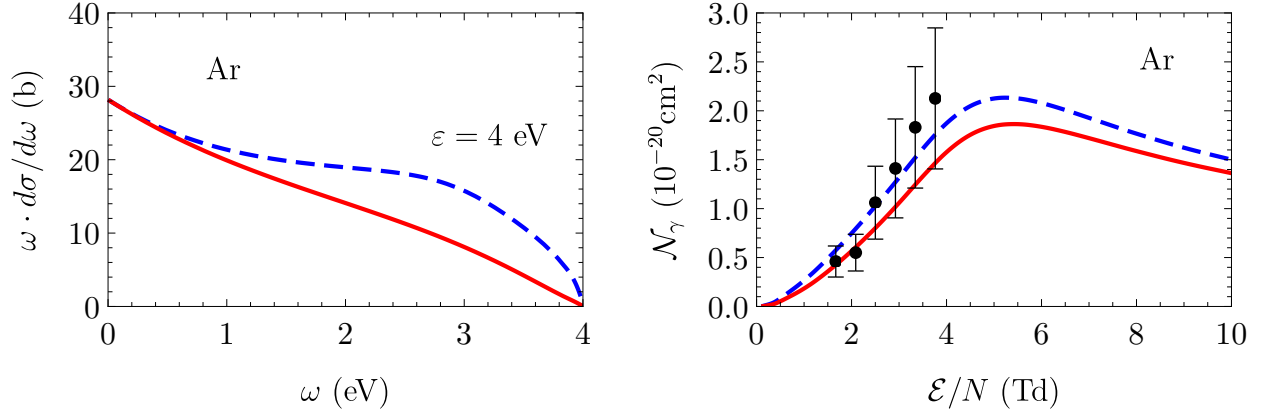


Figure 4. The frequency dependence of $\omega \cdot d\sigma/d\omega$ for scattering of electrons with $\varepsilon = 4$ eV on argon (left figure) and the reduced photon yield as a function of the reduced electric field (right figure). The solid lines correspond to the matrix element given in Eq. (3) and the dashed line to that given in Eq. (21). Experimental data are taken from Ref. [3].

V. PHOTON ANGULAR DISTRIBUTION

From the experimental point of view, it is also interesting to consider the angular distribution of the radiated photons. For this quantity, the exact expression reads (see Appendix)

$$\begin{aligned}
 d\sigma_\gamma &= \frac{d\sigma}{d\omega} \cdot \frac{d\omega d\Omega_{\mathbf{k}}}{4\pi} \cdot [1 + \beta P_2(\cos \theta_{\mathbf{k}})], \quad P_2(y) = \frac{3y^2 - 1}{2}, \\
 \beta &= \frac{1}{2} \left(\sum_{l=0}^{\infty} (l+1) [|M_{l,l+1}|^2 + |M_{l+1,l}|^2] \right)^{-1} \\
 &\times \sum_{l=0}^{\infty} (l+1) \left\{ \frac{6(l+2)}{2l+3} \operatorname{Re}[M_{l+1,l} M_{l+1,l+2}^*] - \frac{l+2}{2l+1} |M_{l,l+1}|^2 - \frac{l}{2l+3} |M_{l+1,l}|^2 \right\}, \quad (22)
 \end{aligned}$$

where $\theta_{\mathbf{k}}$ is the angle between the momentum of the initial electron and the photon momentum, $\frac{d\sigma}{d\omega}$ is given in (3), and $M_{l,l}$ are given in (21). Using Eqs. (5) and (12) we find the asymmetry β at $\omega \ll \varepsilon_i$

$$\begin{aligned}
 \beta(\omega \ll \varepsilon_i) &= \frac{1}{4} \left(\sum_{l=0}^{\infty} (l+1) \sin^2(\delta_l - \delta_{l+1}) \right)^{-1} \\
 &\times \sum_{l=0}^{\infty} (l+1) \sin(\delta_l - \delta_{l+1}) \left\{ \frac{3(l+2)}{2l+3} \sin(\delta_l + \delta_{l+1} - 2\delta_{l+2}) - \frac{5l+4}{2l+1} \sin(\delta_l - \delta_{l+1}) \right\}. \quad (23)
 \end{aligned}$$

Our predictions for the asymmetry β for bremsstrahlung on argon and xenon are shown in Fig. 5. It is seen that the asymmetry is negative for almost all photon and electron energies

considered. In the limit $\omega \rightarrow \varepsilon_i$ the asymmetry tends to $\beta \rightarrow -1$, which can be explained as follows. The matrix element \mathcal{M} of the process can be written as $\mathcal{M} = \mathbf{e} \cdot \mathbf{J}$, where \mathbf{e} is the photon polarization vector and the vector \mathbf{J} is expressed via the momenta \mathbf{p}_i and \mathbf{p}_f of initial and final electrons (see Appendix). Summation over the photon polarizations gives

$$\sum |\mathcal{M}|^2 = |\mathbf{J}|^2 - |\mathbf{n}_k \cdot \mathbf{J}|^2,$$

where $\mathbf{n}_k = \mathbf{k}/k$ and \mathbf{k} is the photon momentum. If $\omega = \varepsilon_i$ then $\mathbf{p}_f = 0$ and $\mathbf{J} \propto \mathbf{p}_i$. Therefore, $\sum |\mathcal{M}|^2 \propto 1 - \cos^2 \theta_k$, which corresponds to $\beta = -1$.

VI. CONCLUSION

In this work, we have carried out a detailed analysis of the bremsstrahlung spectrum at scattering of nonrelativistic electrons on argon and xenon. Predictions obtained by the exact formula (3) differ significantly from the predictions obtained by means of the approximate formula (16) widely used in the literature. This statement is true both for approximate formulas expressed via the transport cross section σ_{tr} and for formulas expressed via σ_{el} . It is shown that the predictions for the photon yield below the luminescence threshold, obtained by means of the exact formula, are in good agreement with the available experimental data.

In the limit $\omega \rightarrow 0$, a rigorous proof is given for the relation between the bremsstrahlung spectrum and the transport scattering cross section. Unlike previous works, this proof does not require any assumptions on the energy dependence of scattering phases.

ACKNOWLEDGEMENTS

We are grateful to A.F. Buzulutskov and E.A. Frolov for valuable discussions.

APPENDIX

In this Appendix we derive the exact formulas for the angular distributions in the process of bremsstrahlung. The differential cross section has the form

$$\begin{aligned} d\sigma &= \frac{\alpha p_f}{\omega p_i} \frac{d\omega d\Omega_{\mathbf{p}_f} d\Omega_{\mathbf{k}}}{(2\pi)^4} |\mathcal{M}|^2, & \mathcal{M} &= \mathbf{e} \cdot \mathbf{J}, \\ \mathbf{J} &= i \int \psi_f^{(-)*}(\mathbf{r}) \mathbf{n} \frac{\partial U}{\partial r} \psi_i^{(+)}(\mathbf{r}), & \mathbf{n} &= \frac{\mathbf{r}}{r}, \end{aligned} \quad (24)$$

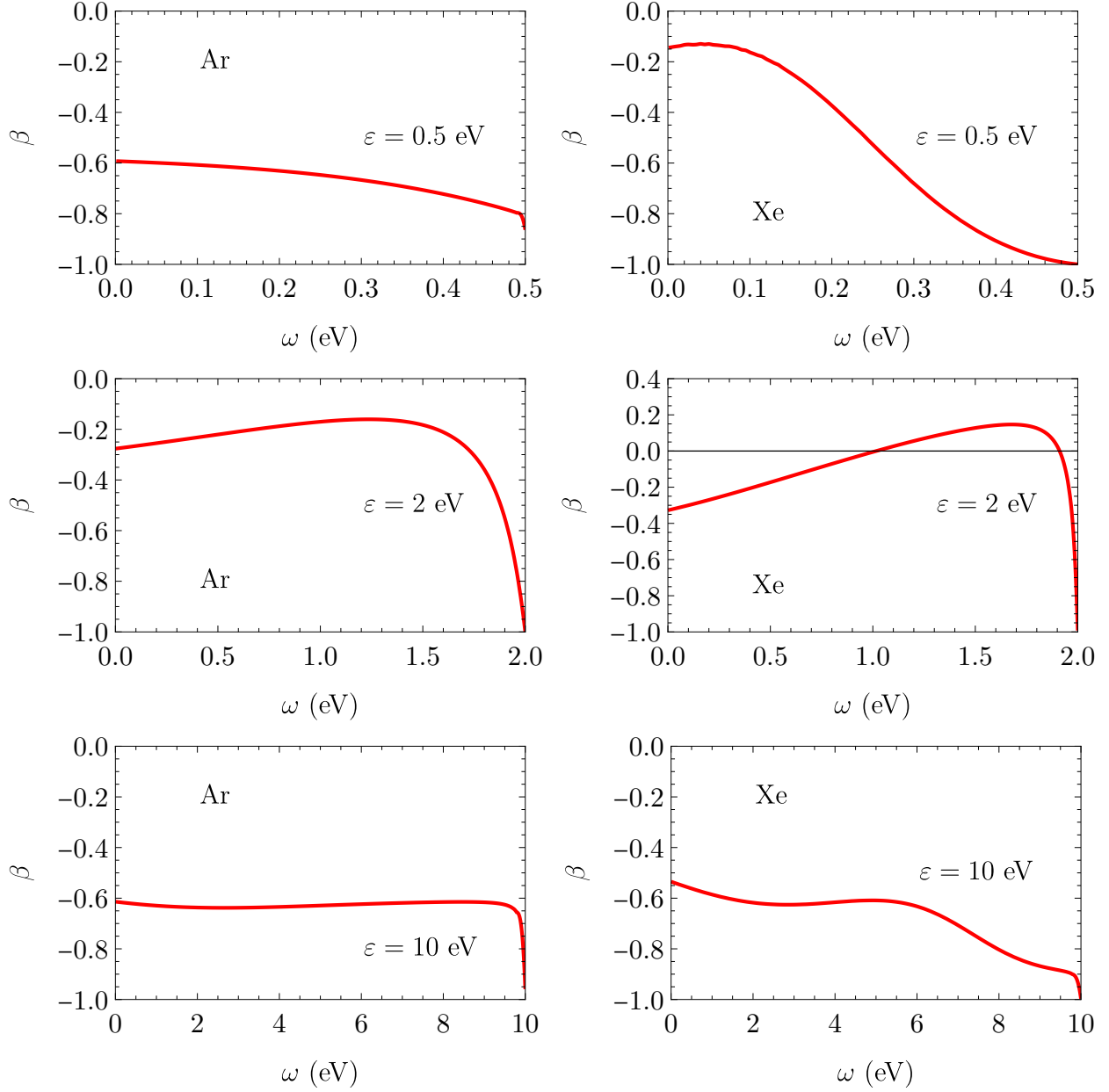


Figure 5. The photon energy dependence of the asymmetry β for bremsstrahlung on argon and xenon at a few electron energies.

where the wave functions $\psi^{(\pm)}(\mathbf{r})$ are given in (1). The matrix element \mathbf{J} is expressed via the vectors $\boldsymbol{\lambda}_i = \mathbf{p}_i/p_i$ and $\boldsymbol{\lambda}_f = \mathbf{p}_f/p_f$, so that we can write \mathbf{J} as

$$\mathbf{J} = \frac{\boldsymbol{\lambda}_i + \boldsymbol{\lambda}_f}{1 + x} A + \frac{\boldsymbol{\lambda}_i - \boldsymbol{\lambda}_f}{1 - x} B, \quad x = \boldsymbol{\lambda}_i \cdot \boldsymbol{\lambda}_f,$$

where

$$A = \frac{1}{2}(\boldsymbol{\lambda}_i + \boldsymbol{\lambda}_f) \cdot \mathbf{J}, \quad B = \frac{1}{2}(\boldsymbol{\lambda}_i - \boldsymbol{\lambda}_f) \cdot \mathbf{J}.$$

Using the recurrent relation for the Legendre polynomials

$$xP_l(x) = \frac{(l+1)P_{l+1}(x) + lP_{l-1}(x)}{2l+1}$$

and the orthogonality relation of the Legendre polynomials we obtain

$$\begin{aligned} A &= \frac{\pi}{2} \sum_{l=0}^{\infty} (l+1) [P_l(x) + P_{l+1}(x)] [M_{l,l+1} - M_{l+1,l}], \\ B &= \frac{\pi}{2} \sum_{l=0}^{\infty} (l+1) [P_l(x) - P_{l+1}(x)] [M_{l,l+1} + M_{l+1,l}], \end{aligned} \quad (25)$$

where $M_{l',l}$ are given in (21).

After summation over the photon polarizations and integration over $\Omega_{\mathbf{k}}$ we obtain the electron angular distribution

$$d\sigma_e = \frac{\alpha}{3\pi^3\omega} \frac{p_i}{p_f} d\omega d\Omega_{\mathbf{p}_f} \left[\frac{|A|^2}{1+x} + \frac{|B|^2}{1-x} \right]. \quad (26)$$

To obtain the photon angular distribution we write

$$\begin{aligned} \int d\Omega_{\mathbf{p}_f} J^a J^{*b} &= a \delta^{ab} + b (\delta^{ab} - 3\lambda_i^a \lambda_i^b), \\ a &= \frac{1}{3} \int d\Omega_{\mathbf{p}_f} |\mathbf{J}|^2, \quad b = \frac{a}{2} - \frac{1}{2} \int d\Omega_{\mathbf{p}_f} |\boldsymbol{\lambda}_i \cdot \mathbf{J}|^2. \end{aligned} \quad (27)$$

Then we use the relations

$$\begin{aligned} \int_{-1}^1 dx \frac{[P_{l+1}(x) + P_l(x)][P_{l'+1}(x) + P_{l'}(x)]}{1+x} &= \frac{2\delta_{ll'}}{l+1}, \\ \int_{-1}^1 dx \frac{[P_{l+1}(x) - P_l(x)][P_{l'+1}(x) - P_{l'}(x)]}{1-x} &= \frac{2\delta_{ll'}}{l+1}, \end{aligned} \quad (28)$$

which can easily be proved. Finally, we have the photon angular distribution

$$\begin{aligned} d\sigma_\gamma &= \frac{d\sigma}{d\omega} \cdot \frac{d\omega d\Omega_{\mathbf{k}}}{4\pi} [1 + \beta P_2(\boldsymbol{\lambda}_i \cdot \mathbf{n}_{\mathbf{k}})], \quad P_2(y) = \frac{3y^2 - 1}{2}, \quad \beta = \frac{b}{a}, \\ a &= \frac{4\pi^3}{3} \sum_{l=0}^{\infty} (l+1) [|M_{l,l+1}|^2 + |M_{l+1,l}|^2], \\ b &= \frac{2\pi^3}{3} \sum_{l=0}^{\infty} (l+1) \left\{ \frac{6(l+2)}{2l+3} \text{Re}[M_{l+1,l} M_{l+1,l+2}^*] - \frac{l+2}{2l+1} |M_{l,l+1}|^2 - \frac{l}{2l+3} |M_{l+1,l}|^2 \right\}, \\ \frac{d\sigma}{d\omega} &= \frac{\alpha}{2\pi^3\omega} \frac{p_f}{p_i} a. \end{aligned} \quad (29)$$

- [2] A. Bondar, et al., [Nucl. Instruments Methods Phys. Res. Sect. A Accel. Spectrometers, Detect. Assoc. Equip.](#) **958**, 162432 (2020).
- [3] E. Borisova and A. Buzulutskov, [Eur. Phys. J. C](#) **81**, 1128 (2021).
- [4] E. Borisova and A. Buzulutskov, [Europhys. Lett.](#) **137**, 24002 (2022).
- [5] C.A.O. Henriques, et al., [Phys. Rev. X](#) **12**, 021005 (2022).
- [6] T. Ohmura and H. Ohmura, [Astrophys. J.](#) **131**, 8 (1960).
- [7] O.B. Firsov and M.I. Chibisov, [ZhETF](#) **39**, 1770 (1960) [[JETP](#) **12**, 1235 (1961)].
- [8] L. M. Biberman and G. Norman, [Usp. Phys. Nauk](#) **91**, 193 (1967) [[Sov. Phys. Uspekhi](#) **10**, 52 (1967)].
- [9] C. Ramsauer, [Ann. Phys.](#) **371**, 546 (1922).
- [10] M. Ashkin, [Phys. Rev.](#) **141**, 41 (1966).
- [11] L. G. D'yachkov and G.A. Kobzev, [J. Phys. B At. Mol. Phys.](#) **16**, 1605 (1983).
- [12] V. Kas'yanov and A. Starostin, [ZhETF](#) **48**, 295 (1965) [[JETP](#) **21**, 193 (1965)].
- [13] V. B. Berestetskii, E. M. Lifshitz, and L. P. Pitaevskii, [Quantum Electrodynamics](#), Pergamon Press (1982).
- [14] M.Y Amusia, [Phys. Rep.](#) **162**, 249 (1988).
- [15] M.Y Amusia, [Bremsstrahlung \(in Russian\)](#), Energoatomizdat (1990).
- [16] O.P. Sushkov, A.I. Milstein, M. Mori, and S. Maekawa, [EPL \(Europhysics Lett.\)](#) **103**, 47003 (2013).
- [17] A.I. Milstein and S.G. Salnikov, [Nucl. Instruments Methods Phys. Res. Sect. B Beam Interact. with Mater. Atoms](#) **313**, 64 (2013).
- [18] W.B. Somerville, [Astrophys. J.](#) **139**, 192 (1964).
- [19] A. Dalgarno and N.F. Lane, [Astrophys. J.](#) **145**, 623 (1966).
- [20] K.L. Bell, N.S. Scott, and M.A. Lennon, [J. Phys. B At. Mol. Phys.](#) **17**, 4757 (1984).
- [21] B. Plenkiewicz, P. Plenkiewicz, and J.-P. Jay-Gerin, [Phys. Rev. A](#) **38**, 4460 (1988).
- [22] H.P. Saha, [Phys. Rev. A](#) **43**, 4712 (1991).
- [23] G. Endrédí and B. Apagyi, [Few-Body Syst.](#) **17**, 199 (1994).
- [24] A.B. McEachran and A.D. Stauffer, [Aust. J. Phys.](#) **50**, 511 (1997).
- [25] W.R. Johnson and C. Guet, [Phys. Rev. A](#) **49**, 1041 (1994).
- [26] J.C. Gibson, et al., [J. Phys. B At. Mol. Opt. Phys.](#) **31**, 3949 (1998).
- [27] M. Kurokawa, et al., [Phys. Rev. A](#) **84**, 062717 (2011).

- [28] V.F. Bratsev, G.B. Deyneka, and I.I. Tupitsyn, *Izv. Acad. Nauk USSR, Ser. Fiz.* **41**, 2655 (1977) [*Bull. Acad. Sci. USSR, Phys. Ser.* **41**, 173 (1977)].
- [29] N.A. Dyatko, I.V. Kochetov, A.P. Napartovich, and A.G. Sukharev, <https://nl.lxcat.net/download/EEDF>.